Damping of the dipole vortex

Xin Li,[1,2] Donna M. Pierce,[1,3] and Henk F. Arnoldus[1,*]

[1]*Department of Physics and Astronomy, Mississippi State University, P.O. Drawer 5167, Mississippi State, Mississippi, 39762-5167, USA*
[2]*e-mail: xl121@msstate.edu*
[3]*e-mail: dmp149@msstate.edu*
**Corresponding author: hfa1@msstate.edu*

Received February 7, 2011; accepted February 14, 2011;
posted February 17, 2011 (Doc. ID 142280); published April 13, 2011

When a circular electric dipole moment, rotating in the x–y plane, is embedded in a material with relative permittivity ε_r and relative permeability μ_r, the field lines of energy flow of the emitted radiation are dramatically influenced by the surrounding material. For emission in free space, the field lines swirl around the z axis and lie on a cone. The direction of rotation of the field lines around the z axis is the same as the direction of rotation of the dipole moment. We found that when the real part of ε_r is negative, the rotation of the field lines changes direction, and hence the energy counter-rotates the dipole moment. When there is damping in the material, due to an imaginary part of ε_r, the cone turns into a funnel, and the density of the field lines diminishes near the location of the source. In addition, all radiation is emitted along the z axis and the x–y plane, whereas for emission in free space, the radiation is emitted in all directions. It is also shown that the displacement of the dipole image in the far field depends on the material parameters and that the shift can be much larger than the shift of the image in free space.

OCIS codes: 080.4865, 260.2110.

1. INTRODUCTION

In the geometric optics limit, the propagation of light from a point source to an observer is represented by optical rays, which are the orthogonal trajectories of the wavefronts. In a linear isotropic homogeneous medium, these optical rays are straight lines, emanating from the location of the source. On the other hand, electromagnetic energy propagates along the field lines of the Poynting vector. It can be shown [1] that in the geometric optics limit, where variations in the radiation field on the scale of a wavelength are neglected, the optical rays coincide with the field lines of the Poynting vector for light propagation in a linear isotropic homogeneous medium. In nanophotonics, near-field optics, and any problem where subwavelength resolution of the energy transport by the radiation field is of interest, this concept of optical rays loses its significance. Energy flows along the field lines of the Poynting vector, and these field lines are, in general, curves rather than straight lines. A prime example is the diffraction of a plane wave of light around an edge of a screen. It was shown for the first time by Braunbek and Laukien [2] that close to the edge, as compared to a wavelength, the field lines of energy transport curve around the edge, and optical vortices appear close to the screen. Optical vortices have been found in numerous other systems, and by far the most studied optical vortices are the vortices in the field of a Laguerre–Gaussian laser beam [3–6]. Recently, it was shown by us [7] that when an electric dipole emits radiation near an interface, singularities and vortices appear in the near field as a result of the interference between the dipole radiation and the light reflected by the interface.

A vortex of a very different nature is the source vortex. Radiation emitted by an electric or magnetic multipole of the order of (ℓ, m), oscillating at angular frequency ω, exhibits a vortex structure [8], except for $m = 0$. The field lines of the Poynting vector swirl around the multipole axis near the source, thereby forming a vortex. The dimension of this multipole vortex is of the order of a wavelength, and at larger distances from the source the field lines go asymptotically over in straight lines. We shall consider electric dipole radiation with $m = 1$. Such radiation is emitted, for instance, during a spontaneous electronic transition in an atom when the magnetic quantum number of the initial state is one higher than the magnetic quantum number of the final state [9]. The corresponding electric dipole moment is a vector that rotates counterclockwise in the x–y plane, when viewed from the positive z axis. Figure 1 shows two field lines of the Poynting vector for the radiation emitted by this dipole. The wavenumber is $k_o = \omega/c$, and the dimensionless Cartesian coordinates are defined as $\bar{x} = k_o x$, etc., so 2π corresponds to one optical wavelength. It can be shown that each field line lies on a cone [10,11], and we see from the figure that the spatial extent of this "dipole vortex" is much smaller than a wavelength.

Another mechanism for the bending of the field lines of energy flow is damping by an embedding medium. When a linear electric dipole ($m = 0$) emits radiation in free space, the field lines of the Poynting vector are straight lines coming out of the dipole. It was recently shown by us [12] that when this dipole is embedded in an absorbing medium, the field lines become curves, and some even form closed loops, starting at the dipole and returning to the dipole. Therefore, damping in a material may lead to a redistribution of the flow of electromagnetic energy rather than just absorption along the path of propagation.

An even more dramatic effect of an embedding medium was reported recently [13]. When the rotating dipole, for which the field lines of emission in free space are shown in Fig. 1, is embedded in a double-negative metamaterial, the

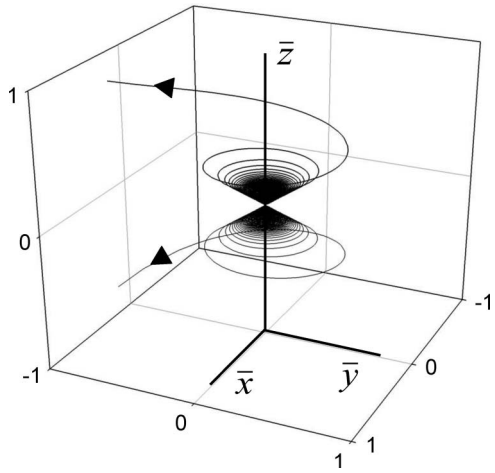

Fig. 1. Two field lines of the Poynting vector for the radiation emitted by a rotating electric dipole moment in free space. The dipole moment rotates counterclockwise in the x–y plane when viewed from the positive z axis. The orientation of the rotation of the field lines around the z axis is the same as the rotation direction of the dipole. The $\bar{x}$ and $\bar{y}$ axes have been lowered for clarity.

direction of rotation of the field lines around the z axis reverses. For such a material, the index of refraction is negative [14].

2. LOCALIZED SOURCE IN A MEDIUM

The optical properties of a linear isotropic homogeneous material can be accounted for by the relative permittivity ε_r and the relative permeability μ_r, and both are complex in general. Due to causality, the imaginary parts of ε_r and μ_r are nonnegative. The index of refraction n is the solution of $n^2 = \varepsilon_r\mu_r$, and we take the solution with $\mathrm{Im}n \geq 0$. This leaves an ambiguity in the definition of n when $n^2 > 0$, and this can only happen when ε_r and μ_r are both positive or both negative. These cases should be considered as limiting cases where the imaginary parts of ε_r and μ_r go to zero [15]. It then follows that we should take $n > 0$ if ε_r and μ_r are both positive and $n < 0$ if ε_r and μ_r are both negative.

We shall assume that a localized source, embedded in the medium, oscillates harmonically at angular frequency ω. The current density of the source can be written as $\mathbf{j}(\mathbf{r},t) = \mathrm{Re}[\mathbf{j}(\mathbf{r})\exp(-i\omega t)]$, with $\mathbf{j}(\mathbf{r})$ being the complex amplitude. The emitted electric field will then have the form $\mathbf{E}(\mathbf{r},t) = \mathrm{Re}[\mathbf{E}(\mathbf{r})\exp(-i\omega t)]$, and a similar expression holds for the magnetic field $\mathbf{B}(\mathbf{r},t)$. The complex amplitude of the electric field is a solution of

$$\nabla\times[\nabla\times\mathbf{E}(\mathbf{r})] - n^2k_o^2\mathbf{E}(\mathbf{r}) = i\omega\mu_o\mu_r\mathbf{j}(\mathbf{r}), \tag{1}$$

and the complex amplitude of the magnetic field follows as

$$\mathbf{B}(\mathbf{r}) = -\frac{i}{\omega}\nabla\times\mathbf{E}(\mathbf{r}). \tag{2}$$

It can be shown by inspection that any solution of Eq. (1), with $\mathbf{B}(\mathbf{r})$ given by Eq. (2), satisfies all four Maxwell equations.

The solution of Eq. (1) can be found in terms of the Green's function for the scalar Helmholtz equation:

$$g(\mathbf{r}) = \frac{e^{ink_or}}{r}. \tag{3}$$

With a similar derivation as in Ref. [16], we obtain

$$\mathbf{E}(\mathbf{r}) = -\frac{i}{3\varepsilon_o\varepsilon_r\omega}\mathbf{j}(\mathbf{r}) + \frac{i\omega\mu_o\mu_r}{4\pi}\int \mathrm{d}^3\mathbf{r}'\mathbf{j}(\mathbf{r}')g(\mathbf{r}-\mathbf{r}') + \frac{i}{4\pi\varepsilon_o\varepsilon_r\omega}\int \mathrm{d}^3\mathbf{r}'[\mathbf{j}(\mathbf{r}')\cdot\nabla]\nabla g(\mathbf{r}-\mathbf{r}'), \tag{4}$$

$$\mathbf{B}(\mathbf{r}) = -\frac{\mu_o\mu_r}{4\pi}\int \mathrm{d}^3\mathbf{r}'\mathbf{j}(\mathbf{r}')\times\nabla g(\mathbf{r}-\mathbf{r}'). \tag{5}$$

The first term on the right-hand side of Eq. (4) comes from moving the differential operators in the third term under the integral sign [17]. Once the complex amplitude of the current density $\mathbf{j}(\mathbf{r})$ of the source is known, Eqs. (4) and (5) give the complex amplitudes of the radiated electric and magnetic fields by the source, embedded in an infinite medium with the parameters ε_r and μ_r and the index of refraction n.

3. ELECTRIC DIPOLE RADIATION

For an electric dipole, located at the origin of the coordinates, the complex amplitude of the current density is $\mathbf{j}(\mathbf{r}) = -i\omega\mathbf{d}\delta(\mathbf{r})$ [18], with $\mathbf{d}$ being a fixed vector, which in general is complex valued. The electric dipole moment of the source is then

$$\mathbf{d}(t) = \mathrm{Re}(\mathbf{d}e^{-i\omega t}). \tag{6}$$

Equations (4) and (5) simplify to

$$\mathbf{E}(\mathbf{r}) = -\frac{1}{3\varepsilon_o\varepsilon_r}\mathbf{d}\delta(\mathbf{r}) + \frac{\mu_r k_o^2}{4\pi\varepsilon_o}\left\{\mathbf{d}g(\mathbf{r}) + \frac{1}{n^2k_o^2}[\mathbf{d}\cdot\nabla]\nabla g(\mathbf{r})\right\}, \tag{7}$$

$$\mathbf{B}(\mathbf{r}) = \frac{i\omega\mu_o\mu_r}{4\pi}\mathbf{d}\times\nabla g(\mathbf{r}), \tag{8}$$

and working out the derivatives of the Green's function yields

$$\mathbf{E}(\mathbf{r}) = -\frac{1}{3\varepsilon_o\varepsilon_r}\mathbf{d}\delta(\mathbf{r}) + \frac{\mu_r k_o^2}{4\pi\varepsilon_o}\left\{\mathbf{d} - (\hat{\mathbf{r}}\cdot\mathbf{d})\hat{\mathbf{r}} + [\mathbf{d} - 3(\hat{\mathbf{r}}\cdot\mathbf{d})\hat{\mathbf{r}}]\frac{i}{nk_or}\left(1 + \frac{i}{nk_or}\right)\right\}g(\mathbf{r}), \tag{9}$$

$$\mathbf{B}(\mathbf{r}) = \frac{n\mu_r k_o^2}{4\pi\varepsilon_o c}(\hat{\mathbf{r}}\times\mathbf{d})\left(1 + \frac{i}{nk_or}\right)g(\mathbf{r}). \tag{10}$$

Here, $\hat{\mathbf{r}} = \mathbf{r}/r$ is the unit vector in the radially outward direction from the location of the dipole to the field point $\mathbf{r}$. The term containing $\delta(\mathbf{r})$ in Eq. (9) is the self field of the dipole. This part of the electric field only exists inside the point dipole, and it will be suppressed from here on.

4. POYNTING VECTOR FOR DIPOLE RADIATION

Energy in an electromagnetic field flows along the field lines of the Poynting vector. For time-harmonic fields in a linear isotropic homogeneous medium, this vector is defined as [19]

$$\mathbf{S}(\mathbf{r}) = \frac{1}{2\mu_o}\mathrm{Re}\left[\frac{1}{\mu_r}\mathbf{E}(\mathbf{r})^* \times \mathbf{B}(\mathbf{r})\right]. \tag{11}$$

Terms that oscillate at twice the optical frequency have been dropped (time-averaged Poynting vector), and this makes $\mathbf{S}(\mathbf{r})$ independent of time. We first write vector $\mathbf{d}$ as $\mathbf{d} = d_o\mathbf{u}$, with $\mathbf{u}\cdot\mathbf{u}^* = 1$, and we introduce

$$P_o = \frac{cd_o^2k_o^4}{12\pi\varepsilon_o}, \tag{12}$$

which equals the power that would be emitted by the same dipole in free space. Then we set $\mathbf{q} = k_o\mathbf{r}$, and therefore $q = k_o r$ is the dimensionless distance between the dipole and the field point. In terms of the variable q, a distance of 2π corresponds to one free-space wavelength. The field lines of the Poynting vector are determined by the direction of $\mathbf{S}(\mathbf{r})$ at the field point $\mathbf{r}$, and not by its magnitude. So if we set

$$\mathbf{S}(\mathbf{r}) = \frac{3P_o}{8\pi r^2}|\mu_r|^2 e^{-2q\mathrm{Im}n}\boldsymbol{\sigma}(\mathbf{q}), \tag{13}$$

then the field lines of $\boldsymbol{\sigma}(\mathbf{q})$ are the same as the field lines of $\mathbf{S}(\mathbf{r})$, because the factor that is split off is positive. Vector $\boldsymbol{\sigma}(\mathbf{q})$ is dimensionless and only depends on the dimensionless representation $\mathbf{q}$ of the field point. We then obtain

$$\begin{aligned}\boldsymbol{\sigma}(\mathbf{q}) = {}& [1-(\hat{\mathbf{r}}\cdot\mathbf{u})(\hat{\mathbf{r}}\cdot\mathbf{u}^*)]\mathrm{Re}\left[\frac{n}{\mu_r}\left(1+\frac{i}{nq}\right)\right]\hat{\mathbf{r}} + \frac{1}{q|n|^2}\left|1+\frac{i}{nq}\right|^2 \\ & \times\{[1-3(\hat{\mathbf{r}}\cdot\mathbf{u})(\hat{\mathbf{r}}\cdot\mathbf{u}^*)]\mathrm{Im}(\varepsilon_r)\hat{\mathbf{r}} + 2\mathrm{Im}[\varepsilon_r(\hat{\mathbf{r}}\cdot\mathbf{u}^*)\mathbf{u}]\}.\end{aligned} \tag{14}$$

In order to see the significance of the various terms in Eq. (14), we first consider the far field. When the distance to the dipole is much larger than a wavelength, we have $q \gg 1$, and Eq. (14) becomes

$$\boldsymbol{\sigma}(\mathbf{q}) \approx [1-(\hat{\mathbf{r}}\cdot\mathbf{u})(\hat{\mathbf{r}}\cdot\mathbf{u}^*)]\mathrm{Re}\left(\frac{n}{\mu_r}\right)\hat{\mathbf{r}}. \tag{15}$$

The factor in square brackets is nonnegative, and it can be shown that $\mathrm{Re}(n/\mu_r)$ is positive [15]. The limiting case where n/μ_r is purely imaginary will not be considered here. Therefore, $\boldsymbol{\sigma}(\mathbf{q})$ is approximately proportional to the radially outward unit vector $\hat{\mathbf{r}}$, and consequently the field lines of the Poynting vector in the far field run approximately radially outward. This also implies that any curving of the field lines can only occur in the near field, e.g., within a distance of about a wavelength from the dipole.

Furthermore, all terms in $\boldsymbol{\sigma}(\mathbf{q})$ are proportional to $\hat{\mathbf{r}}$, except for the term containing the factor $2\mathrm{Im}[\varepsilon_r(\hat{\mathbf{r}}\cdot\mathbf{u}^*)\mathbf{u}]$. Therefore, any curving of the field lines is due to this term. As a function of q, this term is $O(1/q)$ in the far field, as compared to the leading term, which is $O(1)$ and given by Eq. (15). In the near field, however, the term containing $2\mathrm{Im}[\varepsilon_r(\hat{\mathbf{r}}\cdot\mathbf{u}^*)\mathbf{u}]$ is $O(1/q^3)$, and the term containing the factor in braces in Eq. (14) is dominant in the near field. If $2\mathrm{Im}[\varepsilon_r(\hat{\mathbf{r}}\cdot\mathbf{u}^*)\mathbf{u}]$ is nonzero, we may expect a significant curving of the field lines near the source. For instance, for a linear dipole, the vector $\mathbf{u}$ is real, and this factor is proportional to $\mathrm{Im}\varepsilon_r$. Because the imaginary part of ε_r represents damping in the material, the curving of the field lines near the source is a result of absorption in the medium [12].

5. POYNTING VECTOR FOR A CIRCULAR DIPOLE

When the vector $\mathbf{u}$ is taken as $\mathbf{u} = -(\mathbf{e}_x + i\mathbf{e}_y)/\sqrt{2}$, then the dipole moment of Eq. (6) becomes

$$\mathbf{d}(t) = -\frac{d_o}{\sqrt{2}}[\mathbf{e}_x\cos(\omega t) + \mathbf{e}_y\sin(\omega t)]. \tag{16}$$

This dipole moment is a rotating vector in the x–y plane, and the direction of rotation is counterclockwise when viewed from the positive z axis. In the remainder of this paper we shall consider the field lines of energy transport in the radiation emitted by this rotating dipole.

Equation (14) becomes

$$\begin{aligned}\boldsymbol{\sigma}(\mathbf{q}) = {}& \left(1-\frac{1}{2}\sin^2\theta\right)\mathrm{Re}\left[\frac{n}{\mu_r}\left(1+\frac{i}{nq}\right)\right]\hat{\mathbf{r}} + \frac{1}{q|n|^2}\left|1+\frac{i}{nq}\right|^2 \\ & \times\left\{\left[\left(1-\frac{1}{2}\sin^2\theta\right)\hat{\mathbf{r}} + \frac{1}{2}\sin(2\theta)\mathbf{e}_\theta\right]\mathrm{Im}\varepsilon_r \right. \\ & \left. + \mathbf{e}_\phi(\sin\theta)\mathrm{Re}\varepsilon_r\right\},\end{aligned} \tag{17}$$

where (r,θ,ϕ) are the spherical coordinates; $q = k_o r$; and $\hat{\mathbf{r}}$, $\mathbf{e}_\theta$, and $\mathbf{e}_\phi$ are the associated unit vectors. It is easy to show that

$$\mathrm{Re}\left[\frac{n}{\mu_r}\left(1+\frac{i}{nq}\right)\right] > 0, \tag{18}$$

and therefore the first term on the right-hand side is in the radially outward direction. If this would be the only term in $\boldsymbol{\sigma}(\mathbf{q})$, the field lines would be straight lines, coming out of the dipole. The second term on the right-hand side has a part proportional to $\mathbf{e}_\phi(\sin\theta)\mathrm{Re}\varepsilon_r$, and if the imaginary part of ε_r is zero, this is the only additional term. For a given field point $\mathbf{r}$, this gives $\boldsymbol{\sigma}(\mathbf{q})$ a component in the ϕ direction, which is the rotation direction around the z axis. For a small q, this term is $O(1/q^3)$, and this is large in the near field. This term gives the field lines a rotation around the z axis, and the resulting field lines are shown in Fig. 1 for $\varepsilon_r = 1$ (free space). Because $\boldsymbol{\sigma}(\mathbf{q})$ has no θ component for ε_r real, each field line lies on a cone with its axis as the z axis.

When there is damping in the material due to the imaginary part of the permittivity, a term containing $(1-\frac{1}{2}\sin^2\theta)\hat{\mathbf{r}}$ appears, and this term adds to the radially outgoing term. In addition, in the near field, the vector $\boldsymbol{\sigma}(\mathbf{q})$ now has a θ component due to the term containing $\sin(2\theta)\mathbf{e}_\theta$. This will lead to a redirection of the field lines, and hence the field lines will not lie on a cone anymore. In other words, the flow of energy will be redistributed due to the damping.

6. FIELD LINES OF THE POYNTING VECTOR

Let $\mathbf{q}(u)$ be a parameterization of a field line of $\boldsymbol{\sigma}(\mathbf{q})$, with u being a dummy variable. Because at any point $\mathbf{q}$ on a field line the vector $\boldsymbol{\sigma}(\mathbf{q})$ is on the tangent line, the field lines are a solution of

$$\frac{d\mathbf{q}}{du} = \boldsymbol{\sigma}(\mathbf{q}). \tag{19}$$

One field line goes through every point in space, so given an initial point $\mathbf{q}_i$ on a field line, Eq. (19) determines the field line through that point. The field line pictures in this paper are made by numerically solving Eq. (19).

In spherical coordinates (q, θ, ϕ), Eq. (19) becomes

$$\frac{dq}{du} = \boldsymbol{\sigma}(\mathbf{q}) \cdot \hat{\mathbf{r}}, \tag{20}$$

$$q\frac{d\theta}{du} = \boldsymbol{\sigma}(\mathbf{q}) \cdot \mathbf{e}_\theta, \tag{21}$$

$$q\sin\theta\frac{d\phi}{du} = \boldsymbol{\sigma}(\mathbf{q}) \cdot \mathbf{e}_\phi, \tag{22}$$

and the right-hand sides can be found from Eq. (17). This yields the set of equations

$$\frac{dq}{du} = g(q, \theta), \tag{23}$$

$$\frac{d\theta}{du} = \frac{1}{2q^2|n|^2}\left|1 + \frac{i}{nq}\right|^2 \sin(2\theta)\mathrm{Im}\varepsilon_r, \tag{24}$$

$$\frac{d\phi}{du} = \frac{1}{q^2|n|^2}\left|1 + \frac{i}{nq}\right|^2 \mathrm{Re}\varepsilon_r, \tag{25}$$

with

$$g(q,\theta) = \left(1 - \frac{1}{2}\sin^2\theta\right)\left\{\mathrm{Re}\left[\frac{n}{\mu_r}\left(1 + \frac{i}{nq}\right)\right] + \frac{1}{q|n|^2}\left|1 + \frac{i}{nq}\right|^2 \mathrm{Im}\varepsilon_r\right\}. \tag{26}$$

A field line runs into the direction of increasing u. From Eq. (18) and $\mathrm{Im}\varepsilon_r \geq 0$, it follows that the function $g(q, \theta)$ is positive. From Eq. (23) we then see that q increases monotonically along a field line, and because the function $g(q, \theta)$ is larger than $\mathrm{Re}(n/\mu_r)/2$, the value of q increases without bounds along a field line. This implies that field lines start at the dipole ($q = 0$), and run away from the dipole to the far field. Far away from the dipole, q is large, and the right-hand sides of Eqs. (24) and (25) go to zero. Therefore, in the far field, the values of θ and ϕ approach constants, say θ_o and ϕ_o. These are the asymptotic values of θ and ϕ for a large q. Consequently, in the far field, a field line asymptotically approaches a straight line, which runs into the direction (θ_o, ϕ_o).

7. ROTATION OF THE FIELD LINES

Angle ϕ is the angle around the z axis, and we see from Eq. (25) that $d\phi/du$ is positive when $\mathrm{Re}\varepsilon_r$ is positive. Therefore, ϕ increases along a field line, and the field line swirls around the z axis in the positive direction, as in Fig. 1. The rotation direction of the field lines around the z axis is the same as the rotation direction of the dipole moment in the x–y plane. However, when $\mathrm{Re}\varepsilon_r$ is negative, angle ϕ decreases along a field line, and the field line rotates around the z axis opposite to the rotation direction of the dipole moment. We conclude that the vortex reverses its direction of rotation, as compared to the direction of rotation of the dipole, when the real part of the permittivity is negative.

Because q increases monotonically along a field line, we can consider q as the independent variable, rather than u. From Eqs. (23)–(25) we then obtain

$$\frac{d\theta}{dq} = \frac{1}{g(q,\theta)}\frac{1}{2q^2|n|^2}\left|1 + \frac{i}{nq}\right|^2 \sin(2\theta)\mathrm{Im}\varepsilon_r, \tag{27}$$

$$\frac{d\phi}{dq} = \frac{1}{g(q,\theta)}\frac{1}{q^2|n|^2}\left|1 + \frac{i}{nq}\right|^2 \mathrm{Re}\varepsilon_r. \tag{28}$$

We now consider the solution for a small q. When $\mathrm{Im}\varepsilon_r = 0$, we see from Eq. (27) that θ is constant along a field line, and therefore a field line lies on a cone, as in Fig. 1. Then we expand the right-hand side of Eq. (28) in the neighborhood of $q = 0$, and we integrate to obtain $\phi(q)$. This yields

$$\phi(q) = \begin{cases} \mathrm{O}\left(\frac{1}{q^3}\right), & \mathrm{Im}\mu_r = 0 \\ \mathrm{O}\left(\frac{1}{q^2}\right), & \mathrm{Im}\mu_r \neq 0 \end{cases}. \tag{29}$$

For $q \to 0$, the value of $\phi(q)$ goes to ∞ or $-\infty$ rapidly, and this leads to a large number of rotations of a field line around the z axis. Close to the dipole, the number of rotations is so large that the separate turns cannot be distinguished anymore in the neighborhood of the dipole. This can be seen in Fig. 1. When $\mathrm{Im}\varepsilon_r \neq 0$, Eq. (28) becomes

$$\frac{d\phi}{dq} \approx \frac{1}{1 - \frac{1}{2}\sin^2\theta}\frac{1}{\alpha q}, \tag{30}$$

for a small q. Here we have set

$$\alpha = \frac{\mathrm{Im}\varepsilon_r}{\mathrm{Re}\varepsilon_r}. \tag{31}$$

In Eq. (30), θ still depends on q. From Eq. (27) we can find θ for a small q (Section 8), and this yields

$$\phi(q) = \begin{cases} \frac{1}{\alpha}\ln q + \mathrm{O}(1), & z \neq 0 \\ \frac{2}{\alpha}\ln q + \mathrm{O}(1) & z = 0 \end{cases}. \tag{32}$$

For $q \to 0$, the value of $\phi(q)$ goes to $-\infty$ for $\alpha > 0$, so $\mathrm{Re}\varepsilon_r > 0$, and to ∞ for $\mathrm{Re}\varepsilon_r < 0$. This is the same as for the case $\mathrm{Im}\varepsilon_r = 0$. However, the approach of $\phi(q)$ to $\pm\infty$ is now logarithmic, which is much slower than for $\mathrm{Im}\varepsilon_r = 0$. Therefore, the very dense windings around the z axis become much thinner, and this is shown in Figs. 2 and 3. Due to the damping, it appears as if the field lines rotate around the z axis only a few times.

8. FUNNEL VORTEX

When $\mathrm{Im}\varepsilon_r = 0$, field lines lie on a cone, as in Fig. 1, and they are very dense near the location of the dipole. We see from Figs. 2 and 3 that when $\mathrm{Im}\varepsilon_r \neq 0$ the field lines are not only

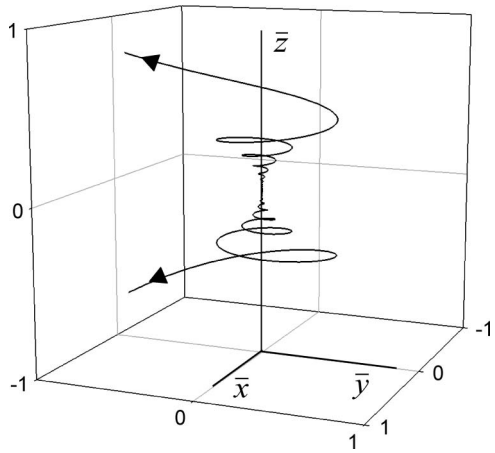

Fig. 2. Two field lines of the Poynting vector for the same dipole as in Fig. 1, but now the dipole is embedded in a medium with $\varepsilon_r = 1 + 0.07i$ and $\mu_r = 1$. Due to the damping, the rotations of the field lines near the dipole are much less dense, as compared to Fig. 1, and the cone shapes of Fig. 1 become funnels.

less dense near the source, but they also do not lie on a cone anymore. It follows from Eq. (25) that ϕ increases or decreases monotonically along a field line. We shall now see ϕ as the independent parameter, and we consider angle θ as a function of ϕ. From Eqs. (27) and (28) we then obtain

$$\frac{\mathrm{d}\theta}{\mathrm{d}\phi} = \frac{1}{2}\alpha \sin(2\theta). \tag{33}$$

The solution of this equation is

$$\tan\theta = e^{\alpha(\phi-\phi_i)} \tan\theta_i, \tag{34}$$

with (θ_i, ϕ_i) the spherical coordinate angles of the initial point. We now consider again the behavior of a field line close to the dipole, so the limit $q \to 0$. It follows from the previous section that $\phi \to -\infty$ for $\alpha > 0$, and to ∞ for $\alpha < 0$, in the limit $q \to 0$. Therefore, $\alpha\phi \to -\infty$, and $\tan\theta$ goes to zero for $q \to 0$. If

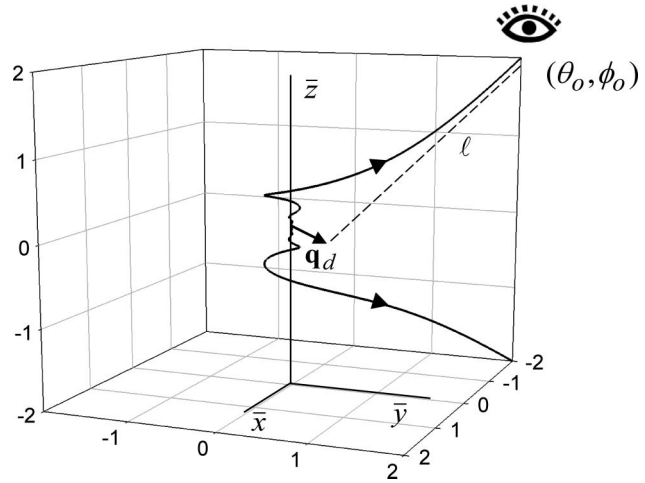

Fig. 3. Same as Fig. 2, but now with $\varepsilon_r = 1 + 0.2i$ and $\mu_r = 1$. We see that due to the increased damping, there are hardly any rotations of the field lines around the z axis left. In the far field, a field line asymptotically approaches a straight line, which is the dashed line ℓ. This line is determined by the observation angles (θ_o, ϕ_o). The intersection of ℓ with the x–y plane is indicated by $\mathbf{q}_d$, which is the virtual displacement vector of the dipole.

the initial point is in the region $z > 0$, so $0 < \theta_i < \pi/2$, this implies that $\theta \to 0$ for $q \to 0$. On the other hand, if the initial point is in the region $z < 0$, so $\pi/2 < \theta_i < \pi$, we have $\theta \to \pi$. For an initial point in the x–y plane, we have $\theta_i = \pi/2$. It follows from Eq. (17) that at any point in the x–y plane, the Poynting vector is in the x–y plane. Therefore, a field line through a point in the x–y plane lies entirely in the x–y plane. So, if $\theta_i = \pi/2$, then $\theta = \pi/2$ for the entire field line. It follows from Eqs. (32) and (34) that $\tan\theta = \mathrm{O}(q)$ for $\alpha \neq 0$ and $\theta_i \neq \pi/2$. Therefore, we have for $q \to 0$

$$\theta(q) = \begin{cases} \mathrm{O}(q), & z > 0 \\ \pi/2, & z = 0 \\ \pi + \mathrm{O}(q), & z < 0 \end{cases}, \tag{35}$$

when $\mathrm{Im}\varepsilon_r \neq 0$. This result can also be derived by expanding the right-hand side of Eq. (27) in a Taylor series in q.

It follows from Eq. (35) that we have $\theta = 0$, $\theta = \pi/2$, or $\theta = \pi$ for $q \to 0$, when the imaginary part of ε_r is finite. Because the radiated energy is emitted along a field line, we come to the remarkable conclusion that due to the damping, all energy is emitted along the z axis or along the x–y plane. This is in sharp contrast to the situation for $\mathrm{Im}\varepsilon_r = 0$, because then the field lines lie on any cone around the z axis. Furthermore, as a result of the damping, the field lines now swirl around on a funnel surface rather than a cone. This funnel shape can clearly be seen in Figs. 2 and 3. Figure 4 illustrates that energy is only emitted along the z axis or along the x–y plane.

9. DISPLACEMENT IN THE FAR FIELD

The solution of Eq. (27) gives θ as a function of the distance q to the dipole. Figure 5 shows graphs of $\theta(q)$ for several initial values of (q_i, θ_i). We see that for $\theta_i < \pi/2$, $\theta(q)$ goes to zero for $q \to 0$, and for $\theta_i > \pi/2$, the value of $\theta(q)$ goes to π, in agreement with Eq. (35). For large q, e.g., in the far field, each curve levels off to a constant θ_o. Similarly, the function $\phi(q)$ diverges

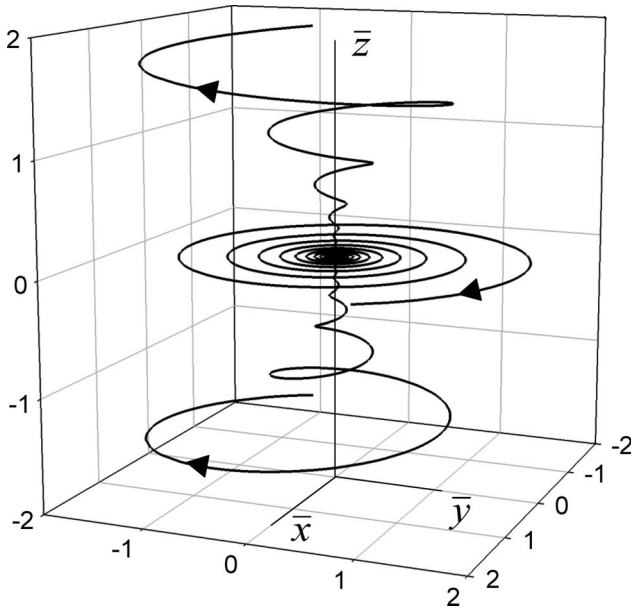

Fig. 4. Three field lines of the Poynting vector for $\varepsilon_r = -1 + 0.1i$ and $\mu_r = 1$, and for the same dipole as in Fig. 1. Because $\mathrm{Re}\varepsilon_r < 0$, the field lines rotate clockwise in the x–y plane (reversal of the vortex). This figure illustrates that energy is only emitted along the z axis or along the x–y plane.

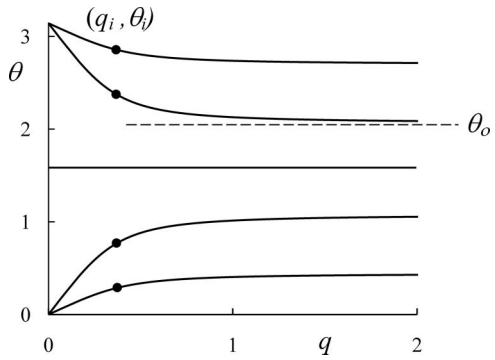

Fig. 5. Graphs of θ as a function q for various initial points (q_i, θ_i), and for $\varepsilon_r = 1 + 0.08i$, $\mu_r = 1$. The initial points for each curve are indicated by a black dot. For a large q, each curve approaches a constant θ_o, representing the value of θ in the far field. The line at $\theta = \pi/2$ represents field lines that lie in the x–y plane.

near the source, and it goes to a constant, ϕ_o, in the far field. At a large distance from the dipole, each field line approaches asymptotically a straight line ℓ, which runs into the direction (θ_o, ϕ_o). This is shown in Fig. 3. Due to the rotation of a field line near the source, this line does not go through the origin of coordinates, and this gives rise to a virtual displacement of the location of the dipole when viewed from the far field [20].

In order to determine line ℓ, we make an asymptotic expansion of $\theta(q)$ for a large q, and for the given observation angles (θ_o, ϕ_o). We write $\theta(q) = \theta_o + \mathrm{O}(1/q)$, and we expand the right-hand sides of Eqs. (27) and (28) up to the leading order in q. Upon integration, we then obtain

$$\theta(q) = \theta_o - Z(\theta_o)\frac{1}{2q}\sin(2\theta_o)\mathrm{Im}\varepsilon_r + \ldots, \tag{36}$$

$$\phi(q) = \phi_o - Z(\theta_o)\frac{1}{q}\mathrm{Re}\varepsilon_r + \ldots, \tag{37}$$

where we have set

$$Z(\theta_o) = \frac{1}{|n|^2\mathrm{Re}(n/\mu_r)\left(1 - \frac{1}{2}\sin^2\theta_o\right)}. \tag{38}$$

The Cartesian coordinates then follow as $\bar{x} = q\sin\theta(q)\cos\phi(q)$, etc. For the field line that runs asymptotically into the direction (θ_o, ϕ_o), we then find

$$\bar{x} = q\sin\theta_o\cos\phi_o + \sin\theta_o\sin\phi_o Z(\theta_o)\mathrm{Re}\varepsilon_r - \cos\theta_o\cos\phi_o Z(\theta_o)\frac{1}{2}\sin(2\theta_o)\mathrm{Im}\varepsilon_r + \ldots, \tag{39}$$

for the $\bar{x}$ coordinate of a point on this field line, and similar expressions hold for the $\bar{y}$ and $\bar{z}$ coordinates. The parameter equation for line ℓ then follows by omitting the ellipses and replacing q by a new parameter t (because this parameter does not represent the distance to the origin anymore).

The resulting equation for line ℓ can be written in a transparent form by adopting a vector notation. The radial unit vector in the direction (θ_o, ϕ_o) is

$$\hat{\mathbf{r}}_o = (\mathbf{e}_x\cos\phi_o + \mathbf{e}_y\sin\phi_o)\sin\theta_o + \mathbf{e}_z\cos\theta_o, \tag{40}$$

and the other two unit vectors associated with the spherical coordinate system are

$$\mathbf{e}_{\theta_o} = (\mathbf{e}_x\cos\phi_o + \mathbf{e}_y\sin\phi_o)\cos\theta_o - \mathbf{e}_z\sin\theta_o, \tag{41}$$

$$\mathbf{e}_{\phi_o} = -\mathbf{e}_x\sin\phi_o + \mathbf{e}_y\cos\phi_o. \tag{42}$$

A point on line ℓ is represented by vector $\mathbf{q} = \bar{x}\mathbf{e}_x + \bar{y}\mathbf{e}_y + \bar{z}\mathbf{e}_z$. We then find

$$\mathbf{q} = t\hat{\mathbf{r}}_o + \mathbf{q}_f \tag{43}$$

as the parameter representation of line ℓ. Here we have introduced the vector

$$\mathbf{q}_f = -\sin\theta_o Z(\theta_o)[\mathbf{e}_{\phi_o}\mathrm{Re}(\varepsilon_r) + \mathbf{e}_{\theta_o}\cos\theta_o\mathrm{Im}(\varepsilon_r)]. \tag{44}$$

Equation (43) has a simple interpretation, as illustrated in Fig. 6. Vector $t\hat{\mathbf{r}}_o$ is a radially outward unit vector. The vectors $\mathbf{e}_{\theta_o}$ and $\mathbf{e}_{\phi_o}$ are perpendicular to $t\hat{\mathbf{r}}_o$, and they can be considered to span a plane perpendicular to $t\hat{\mathbf{r}}_o$, with the end point of $t\hat{\mathbf{r}}_o$ as the origin O' in the plane, as shown in Fig. 6. In other words, the plane is the tangent plane of a sphere with radius t around the dipole and at the location represented by the directions (θ_o, ϕ_o). It follows from Eq. (44) that $\mathbf{q}_f$ lies in this plane. Therefore, if $\mathbf{q}_f$ is drawn from O' as in the figure, then line ℓ intersects this plane under a 90° angle at the end point of vector $\mathbf{q}_f$. Parameter t equals the distance between O' and the dipole. When the plane shown in the figure is in the far field, then line ℓ approximately coincides with the field line that runs into the (θ_o, ϕ_o) direction. Therefore, in the far field this field line crosses the plane at location $\mathbf{q}_f$ and under a 90° angle. Consequently, vector $\mathbf{q}_f$ represents the displacement of this field line as compared to the radially outward direction. This displacement is a result of the rotation of the field line near the source, and as such, this near-field phenomenon should be observable in the far field. The plane in Fig. 6 could be considered the observation plane for the image of the dipole. Although the image of the dipole is a continuous intensity distribution over this plane, the vector $\mathbf{q}_f$ gives a good indication as to where the maximum of the intensity distribution is located [21]. In a recent experiment [22], this shift of the intensity distribution was measured for a dipole in free space.

The positive and negative z axes are field lines, corresponding to the observation directions $\theta_o = 0$ and π. Due to the overall factor $\sin\theta_o$ in Eq. (44), the displacement in these

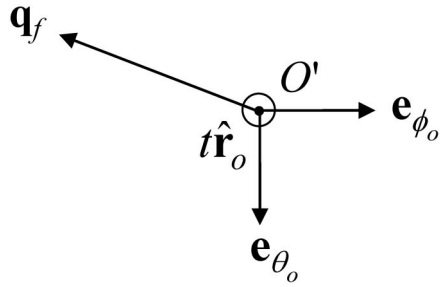

Fig. 6. The observation plane in the direction (θ_o, ϕ_o) is perpendicular to $t\hat{\mathbf{r}}_o$ and spanned by the vectors $\mathbf{e}_{\theta_o}$ and $\mathbf{e}_{\phi_o}$. The asymptote ℓ of the corresponding field line intersects the plane at the location of the displacement vector $\mathbf{q}_f$. Vector $\mathbf{q}_f$ is oriented as shown when the real part of ε_r is positive and $0 < \theta_o < \pi/2$.

directions is zero, as it should be. We also notice that $\mathbf{q}_f$ is independent of the observation angle ϕ_o, as could be expected for a circular dipole. Without damping, so $\mathrm{Im}\varepsilon_r = 0$, vector $\mathbf{q}_f$ is in the ϕ direction. Because $Z(\theta_o)$ is positive, the displacement is in the negative ϕ direction for $\mathrm{Re}\varepsilon_r > 0$ and in the positive ϕ direction for $\mathrm{Re}\varepsilon_r < 0$. This is consistent with the fact that the dipole vortex changes direction with the sign of $\mathrm{Re}\varepsilon_r$. Due to the damping, there is also a displacement in the θ direction. Because $\mathrm{Im}\varepsilon_r \geq 0$, the displacement of the field line is in the negative θ direction for $z > 0$ and in the positive θ direction for $z < 0$. Or we could say that the displacement in the θ direction is away from the x–y plane. It can be checked that the maximum displacement in the ϕ direction occurs for $\theta_o = \pi/2$, e.g., for observation in the x–y plane. The displacement in the θ direction is zero for $\theta_o = 0$, $\pi/2$ and π, and it is maximum for $\theta_o = 54.7°$ and $125.3°$ ($\cos 2\theta_o = -1/3$).

10. APPARENT LOCATION OF THE DIPOLE IN THE *x*–*y* PLANE

The dipole is located at the origin of coordinates in the x–y plane, but when viewed from the far field, it appears as if its position is displaced, as illustrated in Fig. 3. The apparent position of the dipole is at the intersection of line ℓ and the x–y plane. We represent this position by a vector $\mathbf{q}_d$ in the x–y plane, and this vector is found to be

$$\mathbf{q}_d = -\sin\theta_o Z(\theta_o)[\mathbf{e}_{\phi_o}\mathrm{Re}(\varepsilon_r) + \mathbf{e}_{\rho_o}\mathrm{Im}(\varepsilon_r)], \tag{45}$$

where $\mathbf{e}_{\rho_o} = \mathbf{e}_x\cos\phi_o + \mathbf{e}_y\sin\phi_o$ is the radially outward unit vector in the x–y plane. Vector $\mathbf{q}_d$ gives the virtual displacement of the dipole in the x–y plane. The magnitude of the displacement is $q_d = \sin\theta_o Z(\theta_o)|\varepsilon_r|$, and this is

$$q_d = \frac{\sin\theta_o}{|\mu_r|\mathrm{Re}(n/\mu_r)\left(1 - \frac{1}{2}\sin^2\theta_o\right)}. \tag{46}$$

This displacement is of the same order of magnitude as the spatial extent of the vortex, and typically this is of subwavelength dimension, as can be seen in Figs. 1–4. However, the factor $\mathrm{Re}(n/\mu_r)$ in the numerator may become small for certain materials, in which case the displacement may become much larger than a wavelength. This would be the case, for instance, for $\mu_r = 1$, ε_r approximately negative. Then n is approximately positive imaginary, and the displacement is very large.

11. CONCLUSIONS

The field lines of the Poynting vector for the radiation emitted in free space by a circular electric dipole, rotating in the x–y plane, are curves that wind around the z axis, and each field line lies on a cone around the z axis. These flow lines of energy swirl around the z axis in the same direction as the rotation direction of the dipole moment. When the dipole is embedded in a medium with relative permittivity ε_r and relative permeability μ_r, the flow pattern of energy changes dramatically. It is shown that when the real part of ε_r is negative, the rotation of the field lines around the z axis changes direction, and therefore the rotation direction of the energy is opposite to the rotation direction of the dipole moment.

The imaginary parts of ε_r and μ_r give rise to absorption in the surrounding material. It appears that the absorption does not only give rise to a damping of the energy upon propagation but also to a redistribution of the energy flow. When the imaginary part of ε_r is nonzero, the field lines do not lie on a cone anymore, but they swirl around on a funnel-shaped surface. Furthermore, the number of rotations of a field line around the z axis decreases considerably due to the damping, as is most obvious from comparing Figs. 1 and 2. In addition, when $\mathrm{Im}\varepsilon_r \neq 0$ all radiation is emitted along the z axis or in the x–y plane, whereas for a dipole in free space radiation is emitted in all directions.

Far away from the dipole, a field line approaches asymptotically a straight line. Due to the rotation of a field line near the source, this line does not go through the origin of the coordinates. As a result, when viewed from the far field, the field line is displaced as compared to the radially outward direction, and therefore the image of the dipole in the far field is shifted with respect to the radial direction. This displacement is affected by ε_r and μ_r, and the explicit expression for $\mathbf{q}_f$ is given by Eq. (44). In free space, the maximum value of the magnitude of the displacement is $q_f = 2$, which occurs for $\theta_o = \pi/2$, but when the dipole is embedded in a material medium, this can be much larger.

References

1. M. Born and E. Wolf, *Principles of Optics*, 6th ed. (Pergamon, 1980), Chap. 3.
2. W. Braunbek and G. Laukien, "Einzelheiten zur Halbebenen-Beugung," Optik **9**, 174–179 (1952).
3. M. Vasnetsov and K. Staliunas eds. *Optical Vortices*, Horizons in World Physics (Nova Science, 1999), Vol. 228.
4. A. V. Volyar, V. G. Shvedov, and T. A. Fadeeva, "The structure of a nonparaxial Gaussian beam near the focus: II. optical vortices," Opt. Spectrosc. **90**, 93–100 (2001).
5. V. A. Pas'ko, M. S. Soskin, and M. V. Vasnetsov, "Transversal optical vortex," Opt. Commun. **198**, 49–56 (2001).
6. A. V. Volyar, T. A. Fadeeva, and V. G. Shvedov, "Optical vortex generation and Jones vector formalism," Opt. Spectrosc. **93**, 267–272 (2002).
7. X. Li and H. F. Arnoldus, "Electric dipole radiation near a mirror," Phys. Rev. A **81**, 053844 (2010).
8. H. F. Arnoldus, "Vortices in multipole radiation," Opt. Commun. **252**, 253–261 (2005).
9. C. T. Cohen-Tannoudji, B. Diu, and F. Laloë, *Quantum Mechanics* (Wiley, 1977), Vol. 1, p. 838.
10. H. F. Arnoldus and J. T. Foley, "The dipole vortex," Opt. Commun. **231**, 115–128 (2004).
11. J. Shu, X. Li, and H. F. Arnoldus, "Energy flow lines for the radiation emitted by a dipole," J. Mod. Opt. **55**, 2457–2471 (2008).
12. X. Li, D. M. Pierce, and H. F. Arnoldus, "Redistribution of energy flow in a material due to damping," Opt. Lett. **36**, 349–351 (2011).
13. X. Li and H. F. Arnoldus, "Reversal of the dipole vortex in a negative index of refraction material," Phys. Lett. A **374**, 4479–4482 (2010).
14. V. G. Veselago, "The electrodynamics of substances with simultaneously negative values of ε and μ," Sov. Phys. Uspekhi **10**, 509–514 (1968).
15. M. W. McCall, A. Lakhtakia, and W. S. Weiglhofer, "The negative index of refraction demystified," Eur. J. Phys. **23**, 353–359 (2002).
16. H. F. Arnoldus, "Evanescent waves in the near and the far field," in *Advances in Imaging and Electron Physics*, P. W. Hawkes, ed. (Elsevier, 2004), Vol. 132, pp. 1–67.
17. J. van Kranendonk and J. E. Sipe, "Foundations of the macroscopic electromagnetic theory of dielectric media," *Progress in Optics*, E. Wolf, ed. (North-Holland, 1977), Vol. 15, pp. 247–350.

18. J. van Bladel, *Singular Electromagnetic Fields and Sources* (Clarendon, 1991), p. 40.
19. J. D. Jackson, *Classical Electrodynamics*, 3rd ed. (Wiley, 1998), p. 265.
20. H. F. Arnoldus, X. Li, and J. Shu, "Sub-wavelength displacement of the far-field image of a radiating dipole," Opt. Lett. **33**, 1446–1448 (2008).
21. J. Shu, X. Li, and H. F. Arnoldus, "Nanoscale shift of the intensity distribution of dipole radiation," J. Opt. Soc. Am. A **26**, 395–402 (2009).
22. D. Haefner, S. Sukhov, and A. Dogariu, "Spin–Hall effect of light in spherical geometry," Phys. Rev. Lett. **102**, 123903 (2009).